

Redistribution of Spectral Weight in Spin-1/2-Doped Haldane Chains

Stefan Wessel and Stephan Haas

Department of Physics and Astronomy, University of Southern California, Los Angeles, CA 90089-0484
(November 12, 2018)

We study the evolution of the dynamical spin structure factor in a spin-1 antiferromagnetic Heisenberg chain which is randomly doped with spin-1/2 moments. Using stochastic series expansion Quantum Monte Carlo simulations combined with the Maximum Entropy method, we monitor the crossover from the spin-1 chain, dominated by a single resonance at the Haldane energy, to the spin-1/2 chain with a continuum of spinon states which diverges at zero-frequency. Upon increasing the doping level, spectral weight is rapidly transferred from the Haldane peak to lower energies. If the exchange couplings between the spin-1/2 substituents and the spin-1 sites of the host are sufficiently small, finite-frequency bound states are observed below the spin gap for small doping concentrations.

It is well established that antiferromagnetic (AF) spin-1 Heisenberg chains have a low-energy spin gap $\Delta \simeq 0.41J$, leading to properties significantly different from quasi-long-range-ordered spin-1/2 AF Heisenberg chains.¹⁻⁴ The effects of non-magnetic impurities on such low-dimensional quantum spin liquids have been the focus of considerable recent attention. In particular, it was shown that open ends in segmented Haldane chains induce low-energy states below the spin gap,⁵ and that vacancies in AF Heisenberg ladders liberate free spin degrees of freedom in their immediate vicinity^{6,7}. At sufficiently low energies, RKKY-like interactions among these “pruned” spins lead to the formation of networks described by effective models of random spins interacting via random exchange couplings.^{8,9} The effects of substitutions with non-vanishing magnetic moments tend to be more complex, depending on the spins of the dopants as well as on their exchange couplings with the host material.^{10,11} We address this issue by studying the evolution of the dynamical spin structure factor of spin-1 Heisenberg chains when doped with static spin-1/2 moments, and by monitoring the crossover from a completely gapped Haldane spectrum to that of a spin-1/2 chain upon complete substitution.

There have been several experimental and theoretical studies of the effects of spin-1/2 impurities in the spin-1 chain. For example, the substitution of Cu^{2+} for Ni^{2+} in the compound $\text{Ni}(\text{C}_2\text{H}_8\text{N}_2)\text{NO}_2(\text{ClO}_4)$ (NENP) introduces spin-1/2 impurities on the original Ni sites, which have a weak ferromagnetic coupling to the $S = 1$ chain-end spins.¹² On the other hand, substituting Ca^{2+} for Y^{3+} in Y_2BaNiO_5 introduces carriers in the chains which become localized on the oxygen sites between the Ni^{2+} ions. This breaks the superexchange path and replaces it by a direct exchange coupling to the spin-1/2 impurities.¹³ In this latter compound, inelastic neutron scattering experiments found a substantial increase of the spectral function below the Haldane gap, indicating the creation of states below the energy of the spin gap.¹³

Numerical diagonalization and density matrix renormalization group (DMRG) techniques were used to

study the emergence of such impurity-induced low-energy states in the Heisenberg model.^{10,11} The main conclusion of these studies is that localized excited states exist below the Haldane gap as long as the exchange couplings J' between the spin-1/2 and spin-1 sites are small compared to the couplings J between the original spin-1 sites J , namely if $J'/J \lesssim 0.45$. Other works have considered mobile holes.^{14,15} In addition to enhanced low-energy spectral weight in the doped compound, these studies also observe low-temperature spin-glass behavior, due to impurity-induced frustrating ferromagnetic interchain interactions.¹⁶

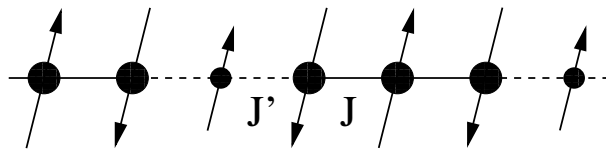


FIG. 1. Spin-1 AF Heisenberg chain with spin-1/2 moments. Exchange couplings between spin-1 sites are indicated by solid lines, whereas the bonds between spin-1/2 and spin-1 sites are denoted by dashed lines.

Here, we concentrate on the static case discussed in Refs.^{10,11} and apply stochastic series expansion Monte Carlo (SSE QMC) simulations¹⁷ in combination with the maximum entropy method¹⁸ to obtain the spectral properties of Haldane chains randomly doped with spin-1/2 sites. This approach allows us to study the evolution of the dynamical spin structure factor upon increasing the spin-1/2 concentration far beyond the limit of low impurity concentration. The doped spin-1 AF Heisenberg chain pictured in Fig. 1 is modeled by a mixed-spin Heisenberg model,

$$H = \sum_{i=1}^N J_i \mathbf{S}_i \cdot \mathbf{S}_{i+1}, \quad (1)$$

where \mathbf{S}_i denotes a spin-1 or spin-1/2 moment. In general, three inequivalent types of bonds exist in a mixed-spin chain: (i) bonds between two spin-1 sites, (ii) bonds

between two spin-1/2 sites, and (iii) bonds between spin-1 and spin-1/2 sites. In the mixed spin model of Eq. 1, we use J as the original coupling of the Haldane chain with $J_i = J$ if S_i and S_{i+1} are both spin-1, and otherwise $J_i = J'$, such that the couplings between spin-1 and spin-1/2 sites are J' . Since we are interested in the generic properties of this problem, in our simulations we concentrate on representative parameter sets.

The significance of J' has been emphasized in Ref.¹⁰ for the case of isolated spin-1/2 impurities. Consider first the two extreme limits $J'/J = 0$ and $J'/J = \infty$. If the spin-1/2 dopants are only weakly coupled to the spin-1 moments of the host, an effective Hamiltonian for the three-site cluster formed by the spin-1 chain-end spins and the impurity spin can be derived, correctly describing the emergence of bound states below the Haldane gap of the spin-1 chain.¹⁰ In the strong coupling limit, the coupling to the remainder of the chain destabilizes the local excitations. A critical coupling ratio $(J'/J)_{crit} = 0.45$ separates these two regimes.^{10,11} Therefore, in the following we discuss separately the cases of weak coupling, which we illustrate with the parameter choice $J' = 0.1J$, and strong coupling, for which we take $J' = J$.

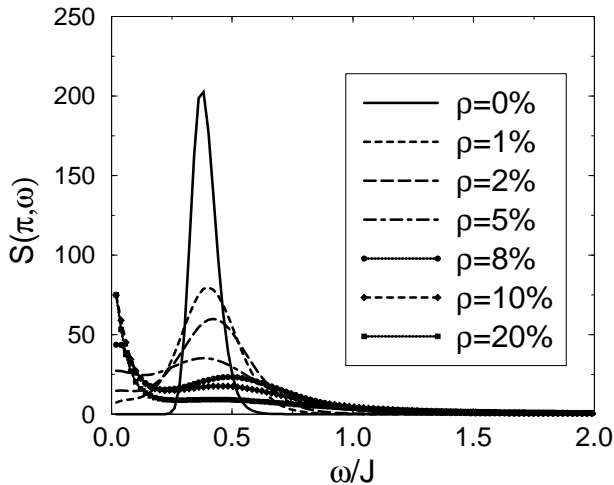


FIG. 2. Spectral function $S(\pi, \omega)$ of the spin-1 chain doped with static spin-1/2 moments for various doping concentration ρ . The exchange couplings between spin-1 and spin-1/2 sites are $J' = 0.1J$ (weak-coupling limit).

In order to observe the evolution of the dynamical spectrum with doping concentration, we have performed SSE QMC simulations¹⁷ and measured the imaginary-time spin-spin correlation function

$$S(\mathbf{k}, \tau) = \frac{1}{N} \sum_{i,j} \exp[-i\mathbf{k}(\mathbf{r}_i - \mathbf{r}_j)] \langle S_i^z(\tau) S_j^z(0) \rangle, \quad (2)$$

considering the dominant AF wave vector $\mathbf{k} = \pi$ by using the Monte Carlo estimator derived in Ref.¹⁹. We studied chains of up to 500 sites for up to 500 realizations of the random distribution of spin-1/2 substituents down to

temperatures $T \gtrsim 0.01J$. The maximum entropy analytical continuation procedure was used to obtain the spectral function $S(\pi, \omega)$ from the impurity-averaged data for the imaginary-time correlation functions.¹⁸

Let us first consider the case $J'/J = 0.1$, where the emergence of localized states below the spin gap is expected from DMRG calculations in the single impurity problem.^{10,11} In Fig. 2 we show the evolution of the spectral function $S(\pi, \omega)$ upon increasing the concentration ρ of spin-1/2 dopants. For the pure spin-1 chain, $\rho = 0$, a dominant resonance is observed at the Haldane gap energy $\omega = \Delta = 0.41J$, consistent with earlier results using similar methods.¹⁸ Upon introducing spin-1/2 sites, the spectral weight of the Haldane peak is strongly suppressed and its width broadens. In addition, a significant amount of spectral weight appears at low but finite energies, indicating the emergence of impurity-induced states below the gap edge. In fact, the shape of the spectral density for $\rho = 0.01$ is consistent with Ref.¹⁰, i.e. bound states with energies of approximately $\alpha J'/2$ and $\alpha 3J'/2$ appear in the low-energy spectrum, where $\alpha = 1.064$ is a renormalization factor for the effective spin-1/2 chain-end spins $\mathbf{S}_{L,R}$ next to the impurity site.²⁰ These localized states are the lowest excited states of the effective Hamiltonian $H_{eff} = \alpha J'(\mathbf{S}_L \cdot \mathbf{S}' + \mathbf{S}' \cdot \mathbf{S}_R)$, where \mathbf{S}' denotes the impurity spin.¹⁰ The maximum entropy method does not allow us to resolve the detailed structure of the spectrum, but clearly indicates the increase of spectral weight at this energy scale with increasing impurity concentration. Upon a further increase of the spin-1/2 concentration beyond $\rho \gtrsim 0.05$, a zero-frequency peak emerges out of these low-energy contributions. Simultaneously, the Haldane peak appears to move towards larger frequencies²¹. The spectrum at larger impurity concentrations ($\rho > 0.2$) exhibits features similar to those of the pure spin-1/2 chain, i.e., a divergence at $\omega = 0$ and no remaining peak structure at the energy of the Haldane gap.

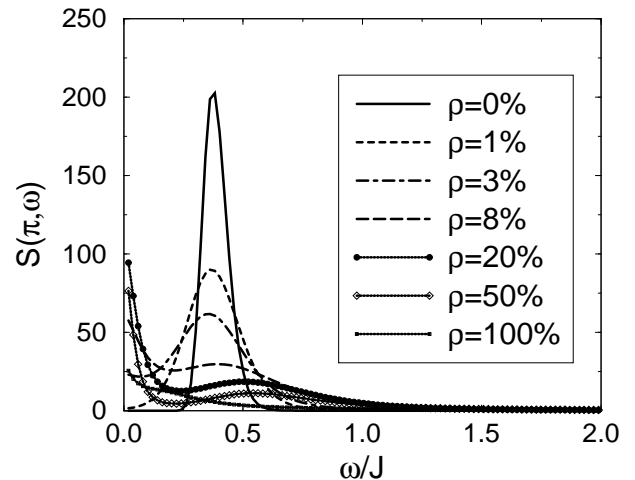


FIG. 3. Same as Fig. 2, but with isotropic exchange coupling constants, $J' = J$, between all spin sites.

Turning to the isotropic case, $J' = J$, DMRG calculations for single spin-1/2 impurities do not exhibit any low-energy states below the Haldane gap.¹⁰ Instead, an extended state with an energy of the order of Δ is reported. We performed SSE QMC simulations for the isotropic case and obtained the dynamical structure factors shown in Fig. 3. Concentrating first on the low-energy properties of this spectral function, we can confirm that in the limit of small impurity concentrations $\rho < 0.06$ no indications of low-lying impurity states are observed, consistent with the DMRG results. Upon further increasing the impurity concentration, a peak appears at zero energy, which develops into the zero-frequency singularity characteristic of the gapless spinon continuum of states in the pure spin-1/2 Heisenberg chain, i.e. $S(\pi, \omega) \propto \sqrt{\ln \omega / \omega}$. Analogous to the discussion of the weak-coupling limit, spectral weight is shifted from the Haldane peak to lower energies. However, in the isotropic case no bound states are observed at finite frequencies below the spin gap. Furthermore, the depletion of the Haldane resonance is less rapid than in the weak-coupling limit, indicating that the presence of weaker bonds has a more dramatic effect on the redistribution of spectral weight than the presence of spin-1/2 substituents.

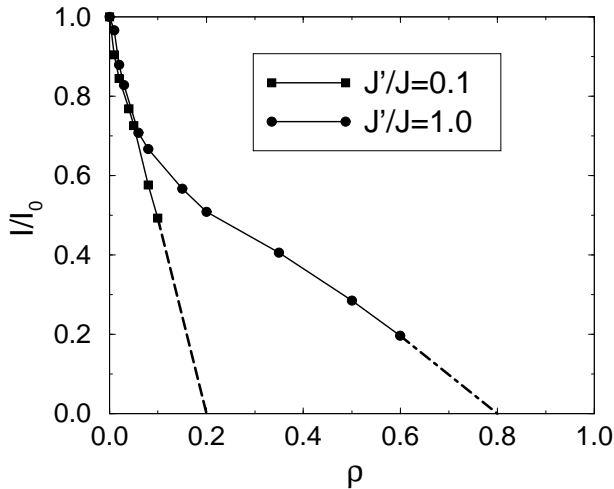


FIG. 4. Spectral weight I of the Haldane peak, normalized to the spectral weight in the clean limit, I_0 . The circles represent the isotropic case $J' = J$, whereas the squares denote the weak-coupling limit at $J' = 0.1J$. The dashed and dot-dashed lines are linear extrapolations.

In order to quantify this statement, the dependence of the spectral weight I at the Haldane energy is plotted in Fig. 4 as a function of the doping concentration. Here, a local Gaussian fit of the spectral function centered around the peak position was used to estimate the spectral weight from the height and the width of the approximant. It is found that in the isotropic case remnants of the Haldane peak can be resolved at much higher spin-1/2 concentrations than in the limit of weak

coupling. For example, at $\rho = 0.5$, the Haldane resonance is still visible in Fig. 3 ($J' = J$), whereas in Fig. 2 ($J' = 0.1J$) this feature cannot be resolved beyond $\rho = 0.2$. This critical value for $J' = 0.1J$ is obtained by a linear extrapolation of I (dashed line shown in Fig. 4). In the case of isotropic couplings the spectral weight of the Haldane peak initially shows a rapid decrease, similar to the weak-coupling limit. However, beyond a doping concentration $\rho \gtrsim 0.06$ at which zero-frequency singularities emerge in the dynamical structure factor (Fig. 3), I decays at a significantly slower rate. It is obviously more difficult to deplete the extended states at the energy of the Haldane gap for isotropic couplings than dissolving the sub-gap bound states in the weak-coupling limit.¹⁰ A linear extrapolation of I (dot-dashed line in Fig. 4) suggests a critical doping concentration $\rho \approx 0.8$ for isotropic couplings. Beyond this concentration the dynamical structure factor resembles that of the pure spin-1/2 AF Heisenberg chain.²²

In conclusion, we have used a combination of stochastic series expansion Quantum Monte Carlo simulations and Maximum Entropy analytical continuation techniques to study the effects of random spin-1/2 substitutions on the dynamical response function of spin-1 AF Heisenberg chains. In the limit of small doping concentrations, the dynamical spin structure factor is found to agree very well with results of earlier DMRG and exact diagonalization studies. If the AF couplings between the spin-1/2 dopants and the spin-1 sites of the host are weak, bound states are formed below the Haldane gap $\Delta \simeq 0.41J$. On the other hand, in the case of isotropic coupling constants there are extended states at the energy of the spin gap. Upon increasing the doping concentration, a proliferation of low-energy states is observed at the expense of the spectral weight of the dominant resonance at $\omega = \Delta$ of the pure spin-1 AF Heisenberg chain. In the limit of weak coupling, the spectral weight of the Haldane peak disappears rapidly. However, for isotropic couplings the transfer of spectral weight to lower energies is more gradual. Here, the gapless spinon continuum spectrum of the pure spin-1/2 AF Heisenberg chain is recovered beyond a critical doping concentration $\rho \approx 0.8$.

We thank B. Normand for useful discussions, and acknowledge financial support by the Petroleum Research Fund, Grant No. ACS-PRF 35972-G6 and by the National Science Foundation, Grant No. DMR 0089882.

¹ F. D. Haldane, Phys. Rev. Lett. **50**, 1153 (1983); Phys. Lett. **93A**, 464 (1983).

² M. Takahashi, Phys. Rev. Lett. **62**, 2313 (1989); Phys. Rev. B **48**, 311 (1993).

³ O. Golinelli, Th. Jolicoeur, and R. Lacaze, Phys. Rev. B **50**, 3037 (1994).

- ⁴ S. Haas, J. Riera, and E. Dagotto, Phys. Rev. B **48**, 3281 (1993).
- ⁵ I. Affleck, T. Kennedy, E.H. Lieb and H. Tasaki, Commun. Math. Phys. **115**, 477 (1988); Phys. Rev. Lett. **59**, 799 (1987); A. K. Kolezhuk, J. Phys.: Condens. Matter **10**, 6795 (1998).
- ⁶ M. Laukamp, G. B. Martins, C. Gazza, A. L. Malvezzi, E. Dagotto, P. M. Hansen, A. C. Lopez, and J. Riera, Phys. Rev. B **57**, 10755 (1998).
- ⁷ G. B. Martins, M. Laukamp, J. Riera, and E. Dagotto, Phys. Rev. Lett. **78**, 3563 (1997).
- ⁸ M. Sigrist and A. Furusaki, J. Phys. Soc. Jpn. **65**, 2385 (1996); T. Fukui, M. Sigrist, and N. Kawakami, Phys. Rev. B **56**, 2530 (1997); E. Westerberg, A. Furusaki, M. Sigrist, and P. A. Lee Phys. Rev. B **55**, 12578 (1997).
- ⁹ S. Wessel, B. Normand, M. Sigrist, and S. Haas, Phys. Rev. Lett. **86**, 1086 (2001).
- ¹⁰ E. S. Sørensen and I. Affleck, Phys. Rev. B **51**, 16115 (1995).
- ¹¹ M. Kaburagi and T. Tonegawa, J. Phys. Soc. Jpn. **63**, 420 (1994).
- ¹² M. Hagiwara, K. Katsumata, I. Affleck, B. I. Halperin, and J. P. Renard, Phys. Rev. Lett. **65**, 3181 (1990); M. Hagiwara, K. Katsumata, H. Hori, T. Takeuchi, M. Date, A. Yamagishi, J. P. Renard, and I. Affleck, Physica B **177**, 386 (1992).
- ¹³ J. F. Ditusa, S.-W. Cheong, J.-H. Park, G. Aeppli, C. Broholm, and C. T. Chen, Phys. Rev. Lett. **73**, 1857 (1994).
- ¹⁴ E. Dagotto, J. Riera, A. Sandvik, and A. Moreo, Phys. Rev. Lett. **76**, 1731 (1996).
- ¹⁵ C. D. Batista, A. A. Aligia, and J. Eroles, Eur. Phys. Lett. **43**, 71 (1998).
- ¹⁶ E. Janod, C. Payen, F.-X. Lannuzel, and K. Schoumacker, cond-mat/0103379.
- ¹⁷ A. W. Sandvik, Phys. Rev. B **59**, R14157 (1999).
- ¹⁸ J. Deisz, M. Jarrell, and D.L. Cox, Phys. Rev. B **48**, 10227 (1993); M. Jarrell and J. E. Gubernatis, Phys. Rep. **269**, 133 (1996).
- ¹⁹ A. W. Sandvik and J. Kurkijärvi, Phys. Rev. B **43**, 5950 (1991).
- ²⁰ S. R. White, Phys. Rev. Lett. **69**, 2863 (1992); E. S. Sørensen and I. Affleck, Phys. Rev. B **49**, 15771 (1994).
- ²¹ Although the SSE QMC allows us to obtain imaginary-time correlation functions with exceptionally small statistical errors, the Maximum Entropy method is known to introduce some inaccuracies in the position and widths of the peaks, in particular at higher frequencies.
- ²² For $J' = J$ the signal of the Haldane peak is beyond $\rho \approx 0.6$. While from the trend of $I(\rho)$ a linear extrapolation yielding $\rho_c \approx 0.8$ appears to be reasonable, it is also possible that remnants of the Haldane peak exist up to $\rho \rightarrow 1$. Unfortunately, this issue is beyond the resolution of the Maximum Entropy method used here.